Neuron
Article

Expression of Cocaine-Evoked Synaptic Plasticity by GluN3A-Containing NMDA Receptors

Tifei Yuan,[1] Manuel Mameli,[2,3] Eoin C. O'Connor,[1] Partha Narayan Dey,[4] Chiara Verpelli,[5] Carlo Sala,[5] Isabel Perez-Otano,[4] Christian Lüscher,[1,6] and Camilla Bellone[1,*]
[1]Department of Basic Neurosciences, Medical Faculty, University of Geneva, 1 rue Michel Servet, CH-1211 Geneva, Switzerland
[2]Institut du Fer à Moulin, 17 rue du Fer à Moulin, 75005 Paris France
[3]Inserm UMR-S 839, 75005 Paris, France
[4]Cellular Neurobiology Laboratory, Centro de Investigacion Medica Aplicada (CIMA) and University of Navarra, Pío XII, 5531008 Pamplona, Spain
[5]CNR Institute of Neuroscience, Department of Pharmacology, University of Milan and Neuromuscular Diseases and Neuroimmunology, Neurological Institute Foundation Carlo Besta, Via Vanvitelli 32, 20129 Milan, Italy
[6]Clinic of Neurology, Department of Clinical Neurosciences, University Hospital of Geneva, 4 rue Gabrielle-Perret-Gentil, 1205 Geneva, Switzerland
*Correspondence: camilla.bellone@unige.ch
http://dx.doi.org/10.1016/j.neuron.2013.07.050

SUMMARY

Drug-evoked synaptic plasticity in the mesolimbic dopamine (DA) system reorganizes neural circuits that may lead to addictive behavior. The first cocaine exposure potentiates AMPAR excitatory postsynaptic currents (EPSCs) onto DA neurons of the VTA but reduces the amplitude of NMDAR-EPSCs. While plasticity of AMPAR transmission is expressed by insertion of calcium (Ca^{2+})-permeable GluA2-lacking receptors, little is known about the expression mechanism for altered NMDAR transmission. Combining ex vivo patch-clamp recordings, mouse genetics, and subcellular Ca^{2+} imaging, we observe that cocaine drives the insertion of NMDARs that are quasi-Ca^{2+}-impermeable and contain GluN3A and GluN2B subunits. These GluN3A-containing NMDARs appear necessary for the expression of cocaine-evoked plasticity of AMPARs. We identify an mGluR1-dependent mechanism to remove these noncanonical NMDARs that requires Homer/Shank interaction and protein synthesis. Our data provide insight into the early cocaine-driven reorganization of glutamatergic transmission onto DA neurons and offer GluN3A-containing NMDARs as new targets in drug addiction.

INTRODUCTION

Cocaine alters excitatory transmission onto synapses of dopamine (DA) in the ventral tegmental area (VTA) within hours of drug exposure. This early form of neuroadaptation persists days after the drug has been cleared from the body (Lüscher and Malenka, 2011). Much experimental evidence suggests that this drug-evoked synaptic plasticity represents a trace that is permissive for widespread circuit adaptations in the mesolimbic system upon chronic drug exposure, eventually leading to addictive behavior (Kauer and Malenka, 2007; Lüscher and Malenka, 2011).

Excitatory synapses in VTA DA neurons contain ionotropic glutamate receptors of the AMPA (AMPARs) and NMDA (NMDARs) type as well as group I metabotropic glutamate receptors (mGluRs-I). AMPARs are the workhorse of synaptic transmission; they are highly mobile and traffic at synapses both constitutively and in an activity-dependent manner (Lüscher and Malenka, 2011; Anggono and Huganir, 2012; Sanz-Clemente et al., 2012). Recent work also suggests activity-dependent trafficking of NMDARs although a unified mechanism for rules of trafficking has not been identified (Kwon and Castillo, 2008; Rebola et al., 2008; Harnett et al., 2009). mGluRs-I are localized perisynaptically but can modulate transmission of AMPARs and NMDARs (Bellone et al., 2008; Lüscher and Huber, 2010; Bellone et al., 2011; Matta et al., 2011).

Cocaine exposure profoundly changes AMPAR transmission at excitatory synapses onto DA neurons in the VTA. The induction of cocaine-evoked synaptic plasticity of AMPAR transmission depends on the concomitant activation of D1Rs (Brown et al., 2010) and NMDARs (Ungless et al., 2001; Engblom et al., 2008). Its expression relies on an exchange of GluA2-containing for GluA2-lacking, Ca^{2+}-permeable AMPARs (CP-AMPARs). Since CP-AMPARs have a higher single-channel conductance, AMPA transmission at resting membrane potentials is potentiated following a single cocaine injection.

One week after a single exposure to cocaine, the drug-evoked plasticity of AMPAR transmission returns to baseline and the mechanisms of this reversal phenomenon have been characterized (Bellone and Lüscher, 2006; Mameli et al., 2007). The recovery of baseline transmission is driven by mGluR1, manifests as a form of long-term depression (LTD), and involves an exchange of CP-AMPARs for Ca^{2+}-impermeable AMPARs (CI-AMPARs, Bellone and Lüscher, 2006). This exchange requires fast and local protein synthesis (Mameli et al., 2007), and reversal of cocaine-evoked synaptic plasticity in the VTA has relevance within the context of drug-seeking behavior (Mameli et al., 2009).

Interestingly, recent evidence suggests that 24 hr after a single cocaine exposure in vivo, the amplitude of unitary

NMDAR-EPSC is reduced (Mameli et al., 2011). This indicates that the increased AMPA/NMDA ratio observed ex vivo in many studies (Ungless et al., 2001; Bellone and Lüscher, 2006) results from a larger AMPAR-mediated component along with a reduced amplitude of NMDAR-mediated component (Mameli et al., 2011). While drug-evoked changes in AMPAR-mediated transmission at excitatory synapses of VTA DA neurons have been extensively studied, little is known about mechanisms that underlie the expression and reversal of plasticity of NMDAR transmission.

NMDARs are heterotetrameric receptors typically containing two GluN1 subunits together with a combination of two GluN2 (A-D) or one GluN2 and one GluN3 (A, B) subunit (Traynelis et al., 2010). Thus, multiple NMDAR subtypes can exist and accumulating evidence indicates that subunit composition determines the receptor's biophysical and pharmacological properties, the quality of synaptic transmission, and the rules for plasticity (Paoletti et al., 2013). Among the GluN2 subunit family, GluN2A and GluN2B subunits are the most abundant in the forebrain. They assemble as canonical heterodimeric or heterotrimeric NMDARs, which have a slow decay time kinetic compared to AMPARs, have strong voltage-dependent Mg^{2+} block, and readily flux Ca^{2+} (Cull-Candy and Leszkiewicz, 2004; Traynelis et al., 2010; Paoletti et al., 2013). Less extensively studied, GluN3A can form noncanonical NMDARs that exhibit distinct properties. Consistent with the mRNA expression in the CNS, GluN3A expression peaks between postnatal days 7 and 10 in the cortex, midbrain, and hippocampus (Al-Hallaq et al., 2002). In hippocampal slices from transgenic mice overexpressing GluN3A, NMDAR-EPSCs show reduced Mg^{2+} sensitivity and the receptors have lower conductance (Roberts et al., 2009). Moreover in neuronal cultures the shift in the reversal potential at different Ca^{2+} concentrations suggest a decreased Ca^{2+} permeability of neurons obtained from GluN3A transgenic mice (Tong et al., 2008). Based on their functional properties derived from investigation in heterologous expression systems, it has been suggested that noncanonical GluN3-containing NMDARs may affect synaptic plasticity and be involved in various neurological diseases (Roberts et al., 2009; Pachernegg et al., 2012). The presence of GluN3A-containing NMDARs has also been described in developmental synapses; however, it remains unknown whether activity-dependent mechanisms can drive their expression at juvenile and adult synapses.

Here we demonstrate that cocaine induces a switch of NMDAR subunit composition at excitatory synapses on DA neurons of the VTA, which reduces NMDAR function. This form of cocaine-evoked synaptic plasticity is expressed by the insertion of GluN3A-containing NMDARs that are quasi-Ca^{2+}-impermeable and necessary for the expression of cocaine-evoked plasticity of AMPARs at these synapses. Moreover, we find that activation of mGluR1 potentiates NMDAR transmission after cocaine exposure and restores basal NMDAR subunit composition via a protein-synthesis-dependent mechanism.

RESULTS

Ca^{2+} Permeability of NMDARs after Cocaine Exposure

At juvenile synapses, when synaptic transmission in the VTA has already reached maturity (Bellone et al., 2011), exposure to cocaine drives insertion of GluA2-lacking AMPARs and decreases NMDAR function at excitatory synapses onto DA neurons (Bellone and Lüscher, 2006; Mameli et al., 2011). In order to investigate whether the source of synaptic Ca^{2+} entry was altered after a single cocaine injection (Figure 1A), we combined two-photon laser microscopy and patch-clamp recordings to image synaptic Ca^{2+} entry in response to activation of AMPARs and NMDARs. All the Ca^{2+} imaging recordings were performed in Mg^{2+}-free solution. As previously described (Ungless et al., 2001; Bellone and Lüscher, 2006), we observed an increase in the AMPAR to NMDAR ratio after cocaine exposure (Figure S1, available online). In parallel we detected synaptic Ca^{2+} transients (Figures 1B–1E) at identified hotspots and measured mixed AMPAR/NMDAR EPSCs (Figure 1F). In the saline condition Ca^{2+} transients and NMDAR-EPSCs were abolished by the selective NMDAR blocker DL-(-)-2-Amino-5-phosphonopentanoic acid (DL-APV, 50 μM, Figures 1D and 1F) while AMPAR-EPSCs were still detectable (Figure 1F). When using the specific CP-AMPAR blocker Philantotoxin 433 (PhTx, 2 μM), we found little or no effect on both the Ca^{2+} transient (Figure 1D) and the AMPAR-mediated EPSCs (data not shown; Bellone and Lüscher, 2006) in recordings from slices of saline-treated animals.

Conversely, in slices from cocaine-treated mice, while DL-APV abolished the NMDA-EPSC (Figure 1F), no significant effect on the Ca^{2+} transient was detected (Figures 1E and 1F). In turn, PhTx or the general AMPARs blocker NBQX abolished the Ca^{2+} transient (Figures 1E and S2). Since all recordings were carried out in a cocktail of blockers for voltage-gated calcium channels (Bloodgood et al., 2009; Bellone et al., 2011) and NBQX left the NMDAR-EPSC untouched (Figure S2), CP-AMPARs were the major source of synaptic Ca^{2+}. Taken together, our data suggest a scenario in which cocaine exposure triggers the insertion of NMDARs that have very low Ca^{2+} permeability (quasi-Ca^{2+}-impermeable NMDARs).

Cocaine Changes the NMDAR Subunit Composition

Ca^{2+} permeability of NMDARs relies largely on the subunit composition (Sobczyk et al., 2005). We next investigated whether cocaine exposure affects the subunit composition of NMDARs at excitatory synapses onto DA neurons. The selective blockers of GluN2A- and GluN2B-containing NMDARs, Zn^{2+} and ifenprodil, respectively (Paoletti, 2011), had differential effects in slices from saline- and cocaine-treated animals. In slices from cocaine-treated mice, NMDAR-EPSCs were strongly inhibited by ifenprodil (3 μM, Figure 2A) while Zn^{2+} inhibition was modest (Figure 2B). These results were inversed in slices of saline-injected mice, where ifenprodil was inefficient but Zn^{2+} strongly inhibited NMDAR-EPSCs. Taken together, these data suggest that the relative contribution of GluN2B subunits increased after cocaine exposure. In agreement with this interpretation, the decay time kinetic, measured as weighted tau (Tw), was slower in slices obtained from cocaine-treated mice, again providing evidence for an increased content of GluN2B subunits (Figure 2C, Bellone and Nicoll, 2007). Notably, we also observed that ifenprodil treatment, while not affecting decay kinetics in saline-treated mice, slowed the decay of NMDAR-EPSCs in cocaine-injected animals (Figure S3A). This is consistent with data showing that in a pure GluN1/GluN2B population, ifenprodil

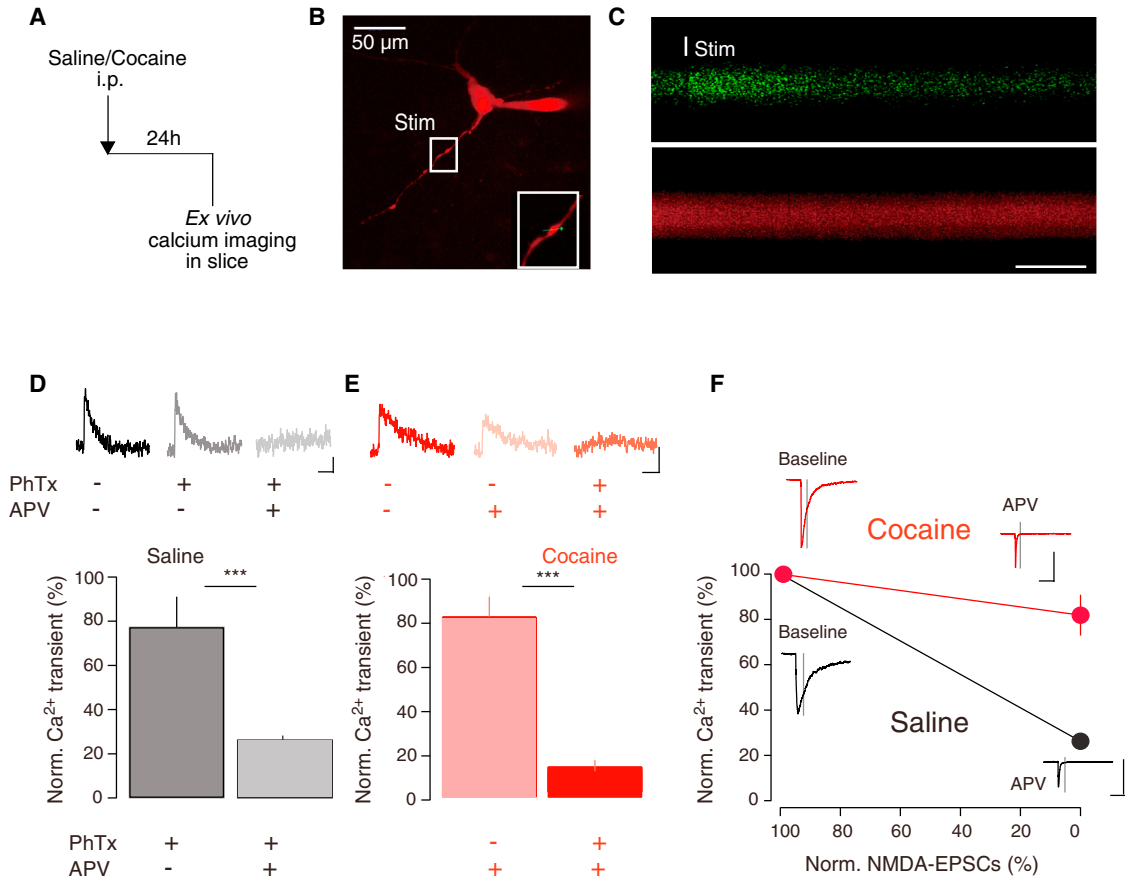

Figure 1. Cocaine Switches Ca^{2+} Permeability from NMDAR to AMPAR Dependent

(A) Injection protocol.

(B) Image of a DA neuron at P18. Box represents the line scan position and "Stim" the position of the stimulating pipette.

(C) Green (Oregon Green BAPTA-1, 100 µM) and red (Alexa FluoRed 594 20 µM) fluorescence collected in a line scan mode during electrical stimulation at synaptic hotspots. Scale bar represents 1 s.

(D) Bottom, bar graph indicating group data for the % of the remaining Ca^{2+} transient. Top, synaptic Ca^{2+} transients shown as ΔG/R fluorescence recorded at −60 mV in Mg^{2+}-free solution. (saline: 77.3% ± 13.8% of baseline in PhTx and 26.2% ± 2.0% of baseline in AP5, $p < 0.001$).

(E) Bottom, bar graph indicating group data for the % of the remaining Ca^{2+} transient. Top, synaptic Ca^{2+} transients shown as ΔG/R fluorescence recorded at −60 mV in Mg^{2+}-free solution from cocaine-treated mice. Scale bar represents 1% ΔG/R and 1 s. Cocaine: 81.9% ± 9.0% of baseline in AP5 and 11.9% ± 5.0% of baseline in PhTx, $p < 0.001$.

(F) Ca^{2+} transient as a function of the normalized NMDAR-EPSCs recorded at −60 mV in Mg^{2+}-free solution at baseline and in the presence of DL-APV. Insets show dual AMPAR-NMDAR EPSCs where the amplitude of the NMDAR component was extracted at 20 ms after the stimulation (gray line). Scale bars represent 200 pA, 50 ms. Error bars represent SEM.

decreases the glutamate dissociation rate (Gray et al., 2011). Zn^{2+} affected the decay time kinetics both in saline- and in cocaine-treated mice (Figure S3B). These data together strongly favor an increase in the GluN2B to GluN2A ratio.

However, a change in the GluN2A/GluN2B ratio is not sufficient to explain the lack of Ca^{2+} permeability observed following cocaine exposure (Figures 1D and 1E). Indeed, both GluN2B and GluN2A containing NMDARs are able to flux Ca^{2+} (Paoletti et al., 2013). To further characterize the NMDAR subunit composition, we plotted the current/voltage (I/V) relationship of NMDAR-EPSCs in slices from cocaine- and saline-treated mice. Remarkably, NMDAR-EPSCs showed decreased outward rectification in slices from mice injected with cocaine 24 hr earlier (Figure 2D). The I/V relationship of NMDAR-EPSCs in saline- and cocaine-treated mice overlap if measured in a Mg^{2+}-free solution, suggesting an altered Mg^{2+} block after cocaine (Figure S3C). This finding could be explained by the presence of GluN2C/D or GluN3 subunits (Cull-Candy and Leszkiewicz, 2004). To examine whether GluN2C/D subunits were involved in the cocaine-evoked plasticity of NMDARs, we applied the recently described selective potentiator of GluN2C/D, CIQ (20 µM, Mullasseril et al., 2010). However, CIQ had no effect on the evoked NMDAR-EPSC, indicating that the GluN2C/D subunit is not part of the NMDAR subunit composition and not implicated in cocaine-evoked plasticity (Figure S3D). To test for the presence of GluN3 we took advantage of GluN3A knockout (KO) mice and used heterozygous (Het) littermate mice as controls. These animals are fertile and follow a Mendelian distribution (Das et al.,

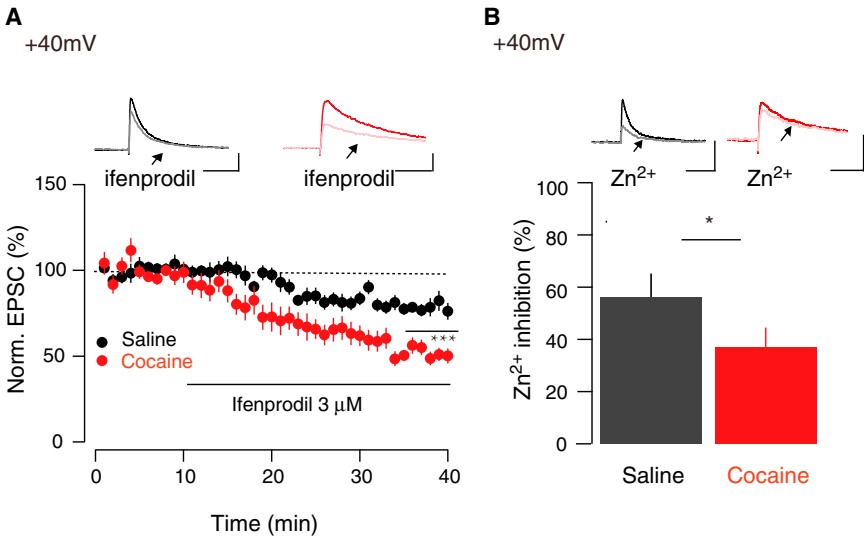

Figure 2. Cocaine Induces Changes in NMDAR Subunit Composition

(A) Sample traces and amplitude versus time plot of NMDAR-EPSCs recorded at +40 mV in the presence of 3 μM ifenprodil. Saline: 77.3% ± 2.6%, n = 9; cocaine, 49.3% ± 1.3%, n = 7. $p < 0.001$.

(B) Sample traces and effects of 300 nM Zn^{2+} on NMDAR-EPSCs recorded at +40 mV. Percentage of inhibition in saline 56.9% ± 9.2%, n = 6; cocaine 37.8% ± 5.9%, n = 6. $p < 0.05$).

(C) Scaled sample traces and decay time for NMDAR-EPSCs recorded at +40 mV (Tw in saline: 104.7 ± 16.2 ms, n = 7; cocaine: 182.1 ± 24.7 ms, n = 7. $p < 0.01$).

(D) Sample traces as well as I-V plots of normalized and averaged NMDAR-EPSCs of VTA DA neurons (−60 mV in saline: −13.7% ± 2.2% of +40 mV, n = 8; cocaine: −27.8% ± 4.5% of +40 mV, n = 17. $p < 0.05$) (−80 mV in Saline: −6.9% ± 1.6% of +40 mV, n = 7; cocaine: −26.5% ± 5.5% of +40 mV, n = 11. $p < 0.05$).

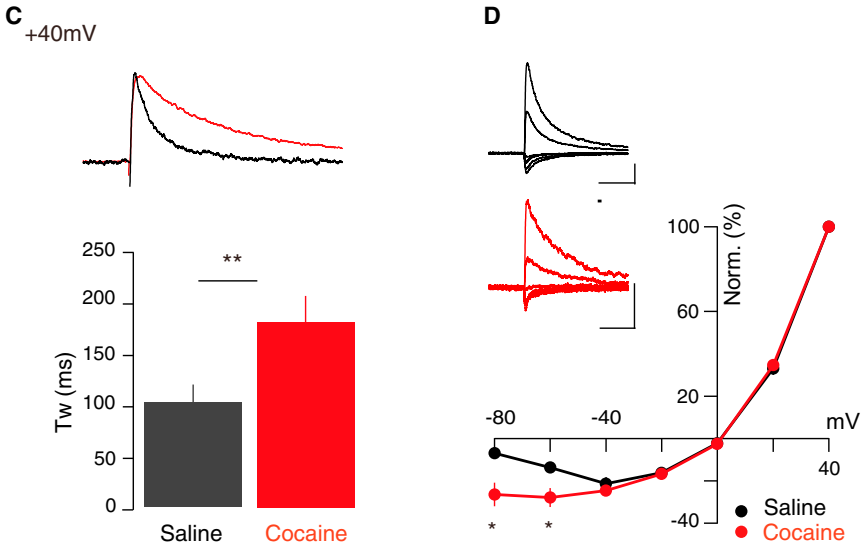

1998). In GluN3A-KO mice, but not in heterozygous controls, cocaine-evoked plasticity of NMDARs was absent, as demonstrated by the normal I/V curve of the NMDAR-EPSCs (Figures 3A and 3B), the sensitivity to ifenprodil, and the decay time kinetic (Figures S4A and S4B). These results suggest that the expression of cocaine-evoked plasticity of NMDAR requires an increase in both the GluN2B and GluN3A content.

GluN3A Gates Cocaine-Evoked Plasticity of AMPARs

Cocaine-evoked synaptic plasticity is induced by NMDAR activation and expressed by a change in both AMPAR and NMDAR receptor subunit composition. To test whether the changes in AMPAR- and NMDAR-mediated transmission are related, we examined cocaine-evoked plasticity of AMPAR transmission (by quantification of the rectification index, Bellone et al., 2011) in mice lacking GluN3A. In heterozygous control mice AMPAR EPSCs were rectifying 24 hr after single cocaine injection, confirming the presence of CP-AMPARs as previously reported in wild-type mice and rats (Bellone and Lüscher, 2006; Argilli et al., 2008). We found no rectification of AMPAR-EPSCs in GluN3A-KO mice, indicating that CP-AMPARs were not present at excitatory synapses onto VTA DA neurons 24 hr after cocaine exposure (Figures 3C and 3D). These findings indicate that cocaine-evoked plasticity of NMDARs, with the insertion of nonconventional GluN3A-containing NMDARs, represents a necessary step for the expression of cocaine-evoked AMPAR plasticity.

Global knockout mice often show compensatory alterations and lack regional specificity. To assess the specific role of GluN3A in cocaine-evoked synaptic plasticity in VTA, we injected unilaterally an adeno-associated viral vector expressing an anti-GluN3A short-hairpin RNA (ShGluN3A) along with GFP into the VTA. We first confirmed in vitro the selectivity of the ShRNA for GluN3A protein (Figure S4C) and we verified its expression in VTA DA cells 2 weeks after the injection (Figures 3E and 3F). We examined cocaine-evoked plasiticty of AMPARs and NMDARs in infected GFP-expressing and noninfected contralateral cells and compared results obtained from saline- and cocaine-treated mice. In contralateral noninfected cells, cocaine drove the insertion of GluN3A-containing NMDARs (Figures 3G, S4D, and S4E) and GluA2-lacking AMPARs (Figure 3I). However, cocaine-evoked plasticity of NMDAR (Figures 3H, S4D, and S4E) or AMPAR (Figure 3J) was not expressed in cells infected with ShGluN3A. The NMDAR I/V curve and AMPAR RI in saline-treated mice was not different from the values obtained in saline noninfected cells, confirming that the ShGluN3A did not affect basal synaptic

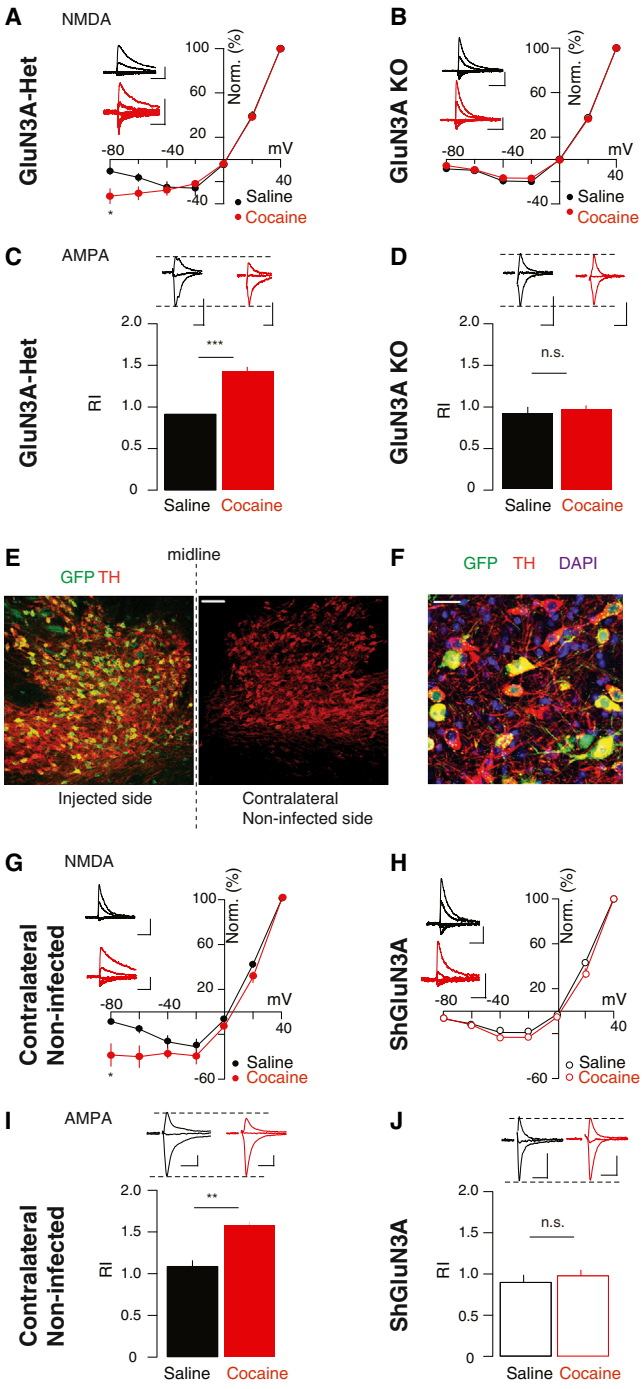

Figure 3. GluN3A Subunit Mediates the Expression of Cocaine-Evoked Plasticity of AMPARs

(A) Sample traces as well as I-V plots of normalized and averaged NMDAR-EPSCs (−60 mV in saline: −16.3% ± 3.8% of +40 mV, n = 6; cocaine: −30.5% ± 6.2% of +40 mV, n = 9. p = 0.09) (−80 mV in saline: −10.4% ± 3.4% of +40 mV, n = 6; cocaine: −33.1% ± 6.9% of +40 mV, n = 9. p < 0.05).

(B) Sample traces as well as I-V plots of NMDAR-EPSCs (−60 mV in saline: −9.8% ± 1.5% of +40 mV, n = 7; cocaine: −9.3% ± 1.2% of +40 mV, n = 9. p = 0.7) (−80 mV in saline: −8.5% ± 2.6% of +40 mV, n = 7; cocaine: −5.6% ± 1.1% of +40 mV, n = 9. p = 0.2). Scale bars represent 50 pA and 100 ms. Group comparison statistic for (A) and (B): effect of drug (saline or cocaine) $F_{(1,23)} = 7.7$, p = 0.01; effect of GluN3A knockout (knockout or not), $F_{(1,23)} = 12.7$, p < 0.01; drug-knockout interaction, $F_{(1,23)} = 8.1$, p = 0.01 (two-way ANOVA).

(C) Sample traces of AMPAR-EPSCs (−70, 0, and +40 mV) and bar graph of rectification index (saline: 0.92 ± 0.06, n = 6; cocaine: 1.44 ± 0.05, n = 9. p < 0.001). Scale bars represent 50 pA and 10 ms.

(D) Sample traces of AMPAR-EPSCs (−70, 0, and +40 mV) and bar graph of rectification index (saline: 0.93 ± 0.07, n = 8; cocaine: 0.98 ± 0.03, n = 8. p = 0.6). Scale bars represent 50 pA and 10 ms. Group comparison statistic for (C) and (D): effect of drug, $F_{(1,23)} = 19.9$, p < 0.001; effect of GluN3A (knockout or not), $F_{(1,23)} = 10.3$, p < 0.01; drug-knockout interaction, $F_{(1,23)} = 20.5$, p < 0.001 (two-way ANOVA).

(E) Immunohistochemistry picture. Scale bar represents 100 μm. Green: GFP; red: TH.

(F) Magnified picture (TH staining, red) by the shRNA-GFP virus (green); blue shows the DAPI staining of the cell nuclei. Scale bar represents 20 μm.

(G) Sample traces as well as I-V plots of normalized and averaged NMDAR-EPSCs (−60 mV in saline: −15.4% ± 3.7% of +40 mV, n = 7; cocaine: −9.9% ± 9.9% of +40 mV, n = 8. p = 0.07) (−80 mV in saline: −8.5% ± 2.3% of +40 mV, n = 7; cocaine: −38.4% ± 10.4% of +40 mV, n = 8. p < 0.05). Scale bars represent 100 pA and 50 ms.

(H) Sample traces as well as I-V plots of normalized and averaged NMDAR-EPSCs (−60 mV in saline: −11.3% ± 1.7% of +40 mV, n = 6; cocaine: −12.4% ± 1.0% of +40 mV, n = 7. p = 0.2) (−80 mV in saline: −6.9% ± 1.0% of +40 mV, n = 6; cocaine: −6.2% ± 1.1% of +40 mV, n = 7. p = 0.6). Group comparison statistic for (G) and (H): effect of drug (saline or cocaine), $F_{(1,23)} = 33.3$, p < 0.001; effect of shRNA-GluN3A infection (knockdown or not), $F_{(1,23)} = 36.9$, p < 0.001; drug-infection interaction, $F_{(1,23)} = 38.2$ p < 0.001. Two-way ANOVA. Scale bars represent 100 pA and 50 ms.

(I) Sample traces of AMPAR-EPSCs (−70, 0, and +40 mV) and bar graph of rectification index of VTA noninfected DA neurons recorded (saline: 1.09 ± 0.07, n = 6; cocaine: 1.58 ± 0.05, n = 9. p < 0.01). Scale bars represent 50 pA and 5 ms.

(J) Sample traces of AMPAR-EPSCs (−70, 0, and +40 mV) and bar graph of rectification index (saline: 0.9 ± 0.09, n = 6; cocaine: 0.98 ± 0.07, n = 6. p = 0.6). Group comparison statistic for (I) and (J): effect of drug (saline or cocaine), $F_{(1,23)} = 17.2$, p < 0.001; effect of shRNA-GluN3A infection (infected or not), $F_{(1,23)} = 28.8$, p < 0.001; drug-infection interaction, $F_{(1,23)} = 9.4$, p < 0.01. Two-way ANOVA. Scale bars represent 50 pA and 5 ms. Error bars represent SEM.

transmission. Taken together, our data indicate that cocaine-evoked plasticity at excitatory synapses onto DA neurons is induced by the insertion of GluN3A-containing NMDARs that contribute to the expression of AMPAR plasticity.

Could knockdown of GluN3A in vivo be sufficient to disrupt cocaine-related behaviors? To test this idea we bilaterally injected the virus expressing ShGluN3A or only GFP in the VTA. Three weeks later, allowing time for virus expression (Figure S5A), we exposed mice to a cocaine-conditioned place preference (CPP) task while simultaneously monitoring locomotor activity. ShGluN3A and control animals showed comparable locomotor sensitization to cocaine (10 mg/kg, i.p.) across conditioning sessions and intact CPP (Figures S5B and S5C). These data are in agreement with previous findings and a model (reviewed in Lüscher and Malenka 2011) in which cocaine-evoked plasticity at excitatory afferents onto VTA DA neurons represents a metaplasticity that is permissive for subsequent downstream changes coupled to long-term adaptive behaviors such as drug seeking, in particular within the nucleus accumbens (Mameli et al., 2009). However, we cannot exclude the possibility that our manipulation lacks the efficiency of infection and cell-type specificity necessary to reveal a role of GluN3A in acute cocaine-related behaviors.

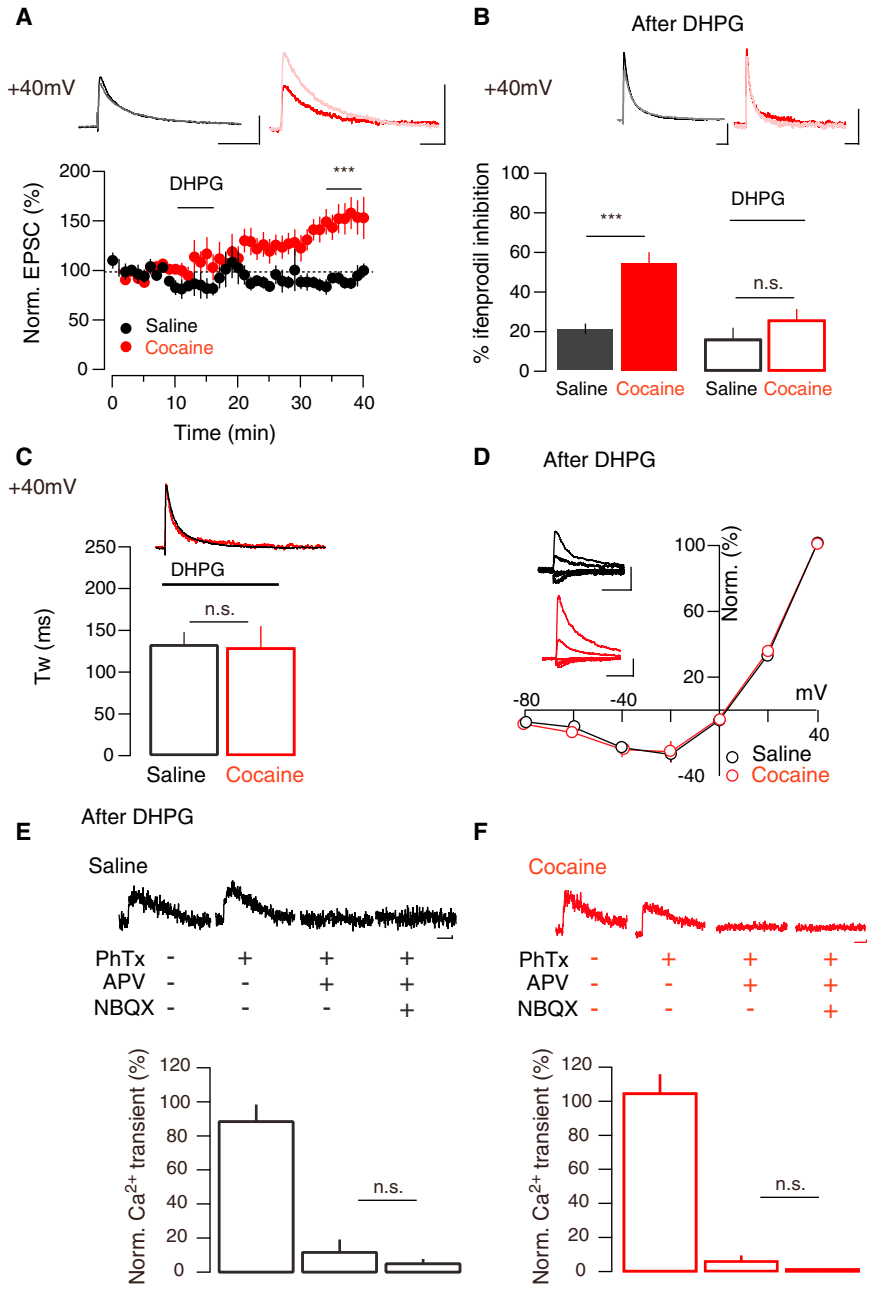

Figure 4. Pharmacological Activation of mGluR1 Restores NMDAR Transmission after Cocaine Exposure

(A) Effect of 5 min application of DHPG on the amplitude versus time plot and sample traces of NMDAR-EPSCs recorded at +40 mV (saline: 92.6% ± 5.4% of baseline, n = 6; cocaine: 170.9% ± 14.4% of baseline, n = 14; $p < 0.001$). Scale bars represent 50 pA and 100 ms.

(B) Sample traces and bar graph representing 3 μM ifenprodil inhibition on NMDAR-EPSCs with or without DHPG pre-incubation (percentage of inhibition in saline: 21.5% ± 2.5%, n = 8; cocaine: 55.0% ± 5.1%, n = 6. $p < 0.001$. Percentage of inhibition in saline slices treated with DHPG: 16.3% ± 5.7%, n = 8; cocaine slices treated with DHPG: 25.8% ± 5.5%, n = 8. $p = 1.0$). Scale bars represent 50 pA and 100 ms. Group comparison statistic for (A) and (B): effect of drug (saline or cocaine), $F_{(1,23)} = 12.6$, $p < 0.01$; effect of DHPG treatment (DHPG treated or not), $F_{(1,23)} = 9.2$, $p < 0.01$; drug-DHPG interaction, $F_{(1,23)} = 6.6$, $p < 0.05$. (Two-way ANOVA.)

(C) Scaled sample traces and decay time for NMDAR-EPSCs recorded at +40 mV after DHPG preincubation (Tw in DHPG-saline: 133.0 ± 15.2 ms, n = 6; DHPG-cocaine: 129.1 ± 26.7 ms, n = 6. $p = 0.9$).

(D) Sample traces as well as I-V plots of normalized and averaged NMDAR-EPSCs of VTA DA neurons in DHPG-incubated slices (−60 mV in DHPG-Saline: −10.4% ± 2.2% of +40 mV, n = 9; DHPG-cocaine: −13.7% ± 3.2% of +40 mV, n = 9. $p = 0.3$) (−80 mV in DHPG-saline: −7.0% ± 1.2% of +40 mV, n = 9; DHPG-cocaine: −8.6% ± 1.2% of +40 mV, n = 9. $p = 0.3$).

(E) Example traces and normalized calcium transient in slices from saline mice after DHPG treatment was 87.8% ± 9.7% after PhTx application, 11.8% ± 7.3% after AP5 application ($p < 0.01$ compared to the PhTx condition), and 5.2% ± 2.6% after NBQX application of baseline ($p = 0.3$ compared to the AP5 condition) (n = 5).

(F) Example traces and normalized Ca^{2+} transient in slices from cocaine mice after DHPG treatment was 104.7% ± 11.2% after PhTx application, 6.2% ± 3.3% after AP5 application ($p = 0.001$ compared to the PhTx condition), and 1.4% ± 0.5% after NBQX application of baseline ($p = 0.2$ compared to the AP5 condition) (n = 5). Scale bars represent 1% ΔG/R and 1 s.

mGluR1 Activation Restores Basal NMDAR Transmission

We have previously shown that mGluR1 activation restores AMPAR-mediated transmission following a single cocaine injection (Bellone and Lüscher, 2006). To test whether mGluR1 activation is also capable of restoring baseline NMDAR-transmission, we applied the mGluR-I agonist DHPG (20 μM) while recording NMDAR-EPSCs and found a substantial increase in the current amplitude only in slices from cocaine-treated mice (Figure 4A). These data are consistent with the removal of low-conductance GluN3A-containing NMDARs. This potentiation of NMDAR-EPSCs occurred concomitantly with a decrease in ifenprodil inhibition (Figure 4B) and was associated with faster decay time kinetics of the evoked NMDAR-EPSCs (Figures 4C, 4D, and S6A). Furthermore, the difference in the I/V relationship between cocaine- and saline-treated mice was absent following DHPG application (Figure 4D). Notably, bath application of DHPG while recording NMDAR-EPSCs at −60mV in cocaine-treated mice induced a small depression, probably caused by the removal of the Mg^{2+}-insensitive, GluN3A-containing NMDARs (Figure S6B). Confirming the removal of nonconventional NMDARs, Ca^{2+} transients measured in Mg^{2+}-free solution after DHPG incubation were mediated by NMDARs and did not differ from saline-treated mice (Figures 4E, 4F, and S6C). Collectively, these data

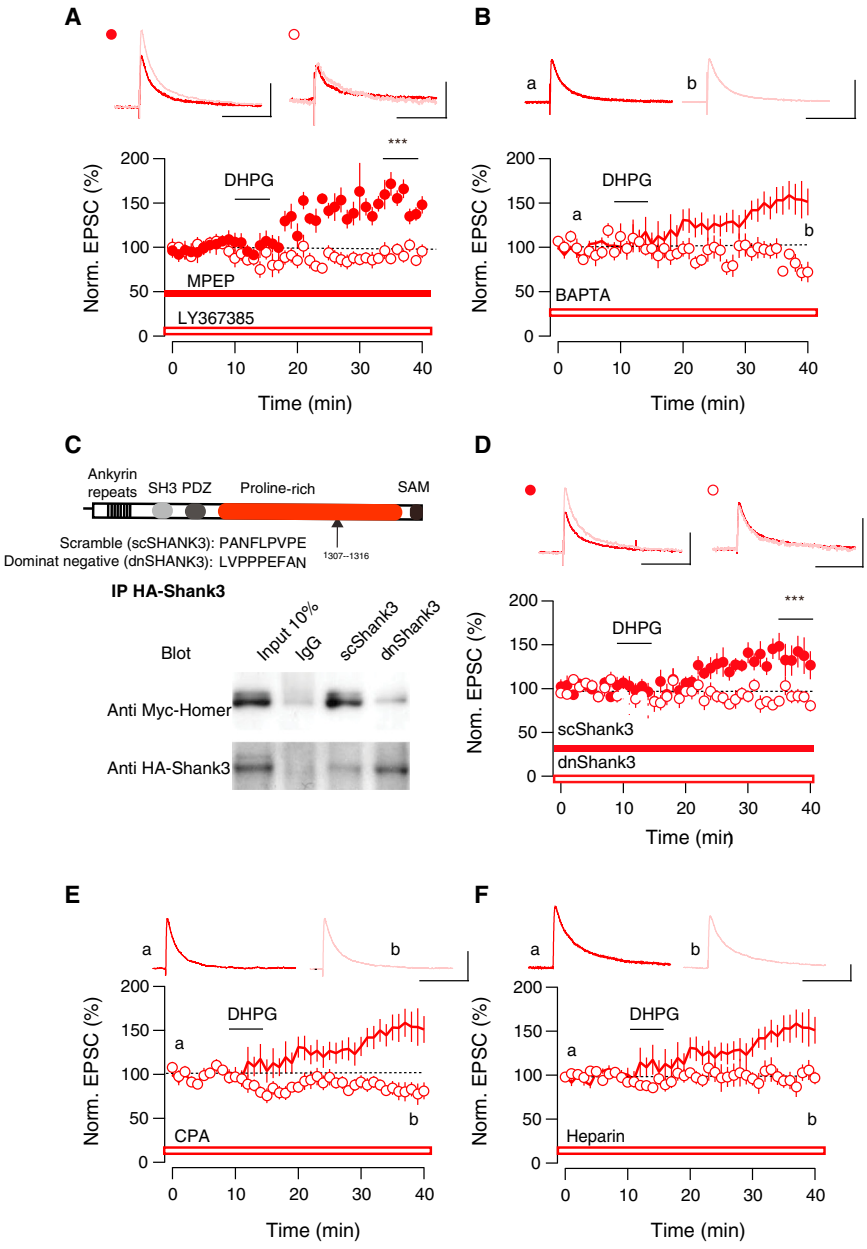

Figure 5. mGluR1-Mediated Potentiation of NMDAR-EPSCs Depends on Ca^{2+} Released from IP_3Rs through Homer/Shank Interaction

(A) In the cocaine group, effect of preincubation of the slices with mGluR1 (LY367385, 25 μM) (open circles) or mGluR5 antagonist (MPEP, 10 μM) (filled circles) on the DHPG-induced potentiation of NMDAR-EPSCs recorded at +40 mV. Top, example traces of the NMDAR-EPSCs. (LY367385: 94.1% ± 6.8% of baseline, n = 12 p = 0.001; MPEP: 148.4% ± 12.8% of baseline, n = 8.)

(B) Effect of application of DHPG on the amplitude versus time plot and sample traces of NMDAR-EPSCs in slices from cocaine group recorded at 40 mV in presence of 10 mM BAPTA in the patch pipette. (78.4% ± 4.0% of baseline, n = 8.)

(C) On top, the design of a peptide containing nine amino acids that disrupts Shank-homer interaction. Immunoprecipitation assay demonstrated the specificity of dnShank3 in disrupting Shank-homer binding in vivo.

(D) Effect of 5 min application of DHPG on the amplitude versus time plot and sample traces of NMDAR-EPSCs in slices from cocaine group recorded at +40 mV in presence of dnShank3 (open circles) or scShank3 (filled circles). (dnShank3: 136.5% ± 7.7% of baseline, n = 6; scShank3 90.4% ± 7.5%, n = 7. p < 0.001.)

(E) In the cocaine group, effect of preincubation of the slices with CPA (30 μM) (open circles) on the DHPG-induced potentiation of NMDAR-EPSCs recorded at +40 mV (80.6% ± 0.9% of baseline, n = 8).

(F) Effect of 5 min application of DHPG on the amplitude versus time plot and sample traces of NMDAR-EPSCs in slices from cocaine group recorded at +40 mV in presence of 2 mg/ml Heparin (IP_3-receptor blocker) in the pipette (97.2% ± 3.4% of baseline, n = 8). Scale bars represent 50 pA and 100 ms. The continuous line in the graphs represent the same data of Figure 4A. Scale bars represent 60 pA and 100 ms. Error bars represent SEM.

suggest that mGluR1 activation is sufficient to re-establish baseline NMDAR transmission by changing the ratio of GluN2B/GluN2A/GluN3A subunits.

Signaling Pathway Underlying mGluR1-Induced Potentiation of NMDARs

Group I mGluRs comprise two receptor subtypes, mGluR1 and mGluR5, both of which are expressed by DA neurons in the VTA. As previously demonstrated for AMPAR-mediated transmission (Mameli et al., 2007), we found that the DHPG-induced potentiation of the NMDAR-EPSCs was mediated by mGluR1 and not mGluR5 since LY367385, but not MPEP, blocked the NMDAR plasticity (Figure 5A). mGluR1 couples to G_q, triggers release of Ca^{2+} from intracellular stores, and can activate various signaling pathways. Since the trafficking of glutamate receptors relies largely on Ca^{2+}-dependent mechanisms, we first investigated the role of postsynaptic Ca^{2+} in the DHPG-induced potentiation of NMDARs. After loading cells with the Ca^{2+} chelator BAPTA, DHPG no longer induced a potentiation of the NMDAR-EPSCs, confirming a necessary role for postsynaptic Ca^{2+}-dependent signaling (Figure 5B).

Shank/Homer protein interaction plays a major role in mGluR1-dependent changes of intracellular signaling that occurs via recruitment of IP_3 receptors (IP_3Rs) to synapses by the Shank/Homer complex (Sala et al., 2005; Hayashi et al., 2009; Verpelli and Sala, 2012). To test whether Shank/Homer is also required for mGluR1-induced potentiation of NMDARs, we designed a dominant-negative peptide mimicking the interaction site of Shank3 with Homer (positions 1307–1316, LVPPPPEEFAN-sequence; Figure 5C). We first characterized

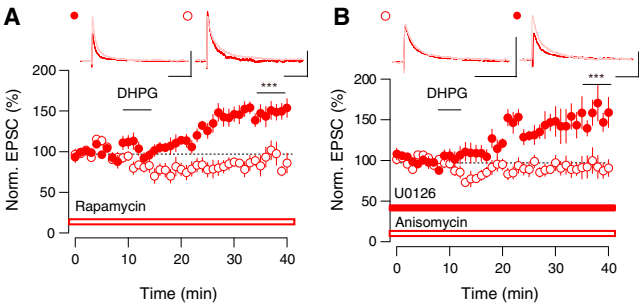

Figure 6. mGluR1-Mediated Potentiation of NMDAR-EPSCs Is Expressed by Fast Protein Synthesis in Response to Activation of the mTOR Pathway

(A) Effect of application of DHPG on the amplitude versus time plot and sample traces of NMDAR-EPSCs in slices from cocaine group recorded at 40 mV in presence of mTOR inhibitor Rapamycin (open circles)(50 nM, 20 min pre-incubation) (rapamycin: 90.9% ± 10.0% of baseline, n = 6; control: 149.2% ± 3.8%, n = 6. $p < 0.001$).

(B) Effect of application of DHPG on the amplitude versus time plot and sample traces of NMDAR-EPSCs in slices from cocaine group recorded at 40 mV in presence of Anisomycin (open circles) (25 μM, 20 min preincubation) or MEK/ERK inhibitor U0126 (open circles) (20 μM, 20 min preincubation) (anisomycin: 92.4% ± 4.6% of baseline, n = 8; U0126: 154.9% ± 12.1%, n = 9. $p < 0.001$). Scale bars represent 60 pA and 100 ms. Error bars represent SEM.

the dominant-negative peptide (dnShank3) and the scrambled control peptide (scShank3) in HEK cells that were transfected with HA-Shank3 and Myc-Homer and the lysate was incubated with either dnShank3 or scShank3. We performed an immunoprecipitation with HA-Shank3 followed by a blot with anti-Myc or anti-HA antibody. We observed that dnShank3 blocked the interaction between Homer and Shank3 protein in vitro (Figure 4C). We then loaded DA neurons in acute brain slices with either dnShank3 or the control scShank3 peptide in the patch pipette and performed whole-cell recordings of pharmacologically isolated NMDAR-EPSCs at +40 mV. While neither peptide affected baseline transmission over a 30 min time period only the dnShank3 abolished DHPG-induced potentiation of NMDARs (Figure 5D), demonstrating that the signaling through the Shank/Homer protein is necessary for mGluR1-dependent plasticity of NMDARs.

mGluR1 activation triggers release of Ca^{2+} from internal stores via activation of the IP_3Rs located on the endoplasmic reticulum (ER, Harnett et al., 2009; Lüscher and Huber, 2010). To investigate the contribution of ER calcium stores, we incubated slices with cyclopiazonic acid (CPA), which selectively blocks the sarcoplasmic-endoplasmic reticulum Ca^{2+}/ATPase pump (Kwon and Castillo, 2008). Slices treated with CPA showed no mGluR1-induced potentiation of the NMDAR-EPSCS (Figure 5E). We next examined the role of IP_3Rs in mediating the release of intracellular Ca^{2+}. Loading cells with the IP_3R blocker heparin efficiently prevented the DHPG-induced potentiation of the NMDAR-EPSCs (Figure 5F). Collectively, these data indicate that the signal transduction between NMDARs and mGluR1s is dependent on intracellular Ca^{2+} signaling.

Downstream of Ca^{2+} signaling, mGluR1 activates both the extracellular signal-regulated kinase (ERK) and the phosphoinositide 3-kinase-Akt-mammalian target of Rapamycin (mTOR). We observed a block of the DHPG-induced potentiation of NMDARs with rapamycin (Figure 6A), but not with the ERK pathway inhibitor U0126 (Figure 6B). The involvement of the mTOR pathway suggests that this form of plasticity is translation dependent, similarly to what has been reported for mGluR-LTD of AMPAR transmission (Mameli et al., 2007). Indeed, preincubation of slices with anysomicin blocked mGluR1-induced plasticity of the NMDAR-EPSCS without affecting baseline transmission (Figure 6C).

Taken together, our data indicate that mGluR1 activation reverses cocaine-evoked plasticity of NMDARs via a Ca^{2+}-dependent signaling transduction pathway, which leads to mTOR activation and protein-synthesis-dependent regulation of NMDARs.

mGluR1 Plasticity Occurs through NMDAR Trafficking

Next we characterized the expression mechanisms of mGluR1-dependent potentiation of NMDAR transmission and asked whether it depended on receptor recruitment and trafficking. In fact, phosphorylation of the receptor, in particular via PKC activation, plays a major role in NMDAR trafficking at many synapses (Lau and Zukin, 2007). The PKC pathway is activated by a rise in intracellular Ca^{2+} concentration; we therefore tested whether this kinase would play a role in the mGluR1-induced potentiation of NMDARs. We incubated slices with a specific PKC inhibitor, chelerythrine, which blocked the potentiation of NMDA induced by DHPG application (Figure 7A). In other systems, PKC has been shown to promote NMDAR trafficking via SNARE-dependent exocytosis (Lau et al., 2010). To test the hypothesis that mGluR1 activation leads to the delivery of NMDARs at synapses, we dialyzed tetanus-toxin (TeTx) through the patch pipette, which allows cleavage of the VAMP2 protein and therefore blocks exocytosis. While the heat-inactivated (95 degrees for 1 hr) toxin did not affect the mGluR1-induced potentiation of NMDARs, TeTx blocked the plasticity (Figure 7B). To confirm this result, we took advantage of a peptide that mimics the C-terminal tail of SNAP-25 protein and interferes with formation of the SNARE complex (Lau et al., 2010). The SNAP-25 peptide blocked the mGluR-potentiation of NMDARs when loaded into the cell, while a scrambled control peptide was without effect (Figure 7C).

DISCUSSION

Here we elucidate the expression mechanism that underlies the changes in NMDAR transmission at excitatory synapses on VTA DA neurons, evoked by a single cocaine injection. We provide evidence for the exchange of Ca^{2+}-permeable for quasi-Ca^{2+}-impermeable NMDARs that occurs together with a switch from CI-AMPARs to CP-AMPARs. We identify GluN3A as the determinant subunit for the Ca^{2+} permeability of these nonconventional NMDARs and show that GluN3A-containing NMDARs are necessary for the expression of cocaine-evoked plasticity in the VTA. Importantly, together with previous studies (Bellone and Lüscher, 2006; Mameli et al., 2007) we find mGluR1 signaling as the common molecular mechanism responsible for restoring basal excitatory transmission (AMPAR and NMDAR) after cocaine exposure (see Figure 8 for NMDARs and Bellone and Lüscher, 2012 for AMPARs). Our data therefore strongly

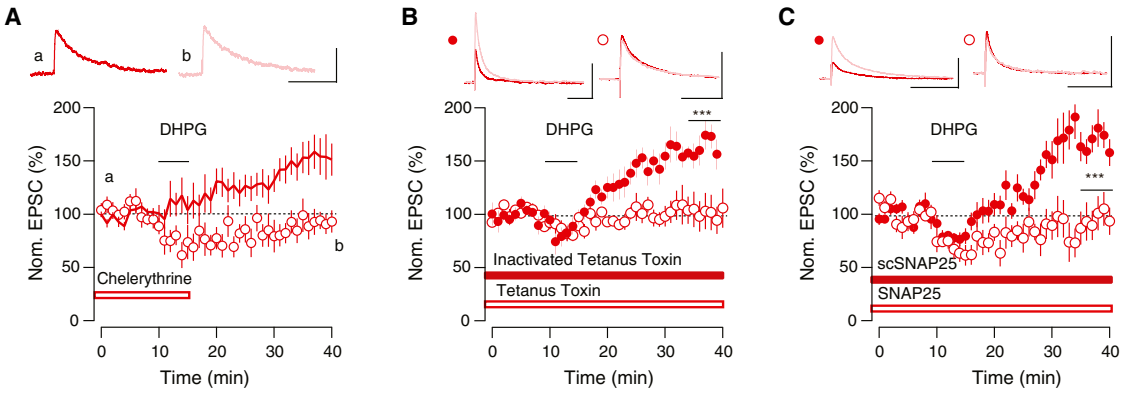

Figure 7. mGluR1-Mediated Potentiation of NMDAR-EPSCs Requires PKC Activation and NMDAR Trafficking via SNARE-SNAP25 Interaction

(A) Effect of application of DHPG on the amplitude versus time plot and sample traces of NMDAR-EPSCs in slices from cocaine group recorded at +40 mV in presence of PKC blocker Chelerythrine (10 μM, 20 min preincubation) (open circles) (Chelerythrine: 91.8% ± 1.0% of baseline, n = 8). Scale bars represent 60 pA and 200 ms. The continuous line represents the same data shown in Figure 2B.

(B) Effect of application of DHPG on the amplitude versus time plot and sample traces of NMDAR-EPSCs in slices from cocaine group recorded at 40 mV in presence of the active (open circles) or inactive (open circles) form of the tetanus toxin in the pipette (100 ng/ml) (tetanus toxin: 100.3% ± 4.1% of baseline, n = 9; heat-inactivated tetanus toxin (tetanus toxoid): 163.7% ± 4.2%, n = 7. $p < 0.001$). Scale bars represent 100 pA and 200 ms.

(C) Effect of application of DHPG on the amplitude versus time plot and sample traces of NMDAR-EPSCs in slices from cocaine group recorded at 40 mV in presence of the short SNAP-25 interfering peptide (SNAP-25 c-term, 300 μM) versus the scramble peptide on mGluR-LTP (SNAP-25 peptide: 96.3% ± 6.4% of baseline, n = 7; scramble peptide: 168.5% ± 10.0%, n = 10. $p < 0.001$). Scale bars represent 100 pA and 200 ms. Error bars represent SEM.

support the idea that mGluR1 signaling controls the GluN3A content at excitatory synapses onto DA neurons.

NMDARs are heteromeric receptors that can be classified based on their subunit composition. Three subunit families have been cloned so far based on sequence homology: GluN1, GluN2 (A-D), and GluN3 (A-B). While GluN1 is the obligatory subunit, GluN2 and GluN3 subunits determine the functional heterogeneity of NMDARs (Monyer et al., 1994; Traynelis et al., 2010). The existence of specific modulators for GluN2 subunits, such as ifenprodil or Zn^{2+}, facilitates the study of the functional properties of NMDARs (Paoletti, 2011). Pharmacological GluN3A modulators are not available, but data derived from expression systems indicate that the presence of GluN3A is responsible for low channel conductance, low Ca^{2+} permeability, and low Mg^{2+} sensitivity (Das et al., 1998; Perez-Otano et al., 2001; Tong et al., 2008; Paoletti et al., 2013). Both diheteromeric and triheteromeric complexes formed by GluN1 with one or two different GluN2 subunits exist (Al-Hallaq et al., 2007; Gray et al., 2011). Moreover, transgenic animal models infer the existence of triheteromeric GluN1/GluN2/GluN3 receptors (Das et al., 1998; Tong et al., 2008). Recordings of DA neurons of the VTA after cocaine exposure lead to the observation of decreased NMDAR-EPSCs (Mameli et al., 2011) along with very low Ca^{2+} permeability and low Mg^{2+} sensitivity, suggesting the insertion of GluN3A-containing NMDARs at VTA DA synapses. In addition, the change in ifenprodil and Zn^{2+} sensitivity, concomitant with an increase in the decay time kinetics, indicates a switch in the relative contribution of GluN2A and GluN2B following cocaine exposure. Since ifenprodil partially inhibits NMDAR-EPSCs in saline-treated mice, we cannot exclude the presence of GluN1/GluN2A/GluN2B triheteromers in baseline conditions at juvenile synapses. Taken together, our data are best explained by a model in which cocaine drives the insertion of triheteromeric GluN1/GluN2B/GluN3A containing complexes that replace GluN1/GluN2A diheteromers and GluN1/GluN2A/GluN2B triheteromers.

The cocaine-driven subunit switch of NMDAR subunits mimics observations made during development (Williams et al., 1993; Sheng et al., 1994; Sanchez et al., 2010). During the first postnatal week, GluN2B-containing NMDARs are replaced by GluN2A-containing ones in most glutamatergic synapses, including excitatory synapses onto VTA DA neurons (Sheng et al., 1994; Sans et al., 2000; Bellone and Nicoll, 2007). This postnatal subunit switch is activity dependent, regulates AMPAR expression, and depends on the activation of group I mGluRs both in the hippocampus and in the VTA (Bellone et al., 2011; Matta et al., 2011; Gray et al., 2011). The GluN3A subunit also has a developmental distribution profile (Wong et al., 2002; Henson et al., 2010). Because of its expression profile, GluN3A may represent a molecular break for synaptic maturation (Roberts et al., 2009). In agreement with this idea, GluN3A overexpression decreases spine density and attenuates LTP induction at CA1 hippocampal synapses (Roberts et al., 2009). Moreover, deletion of GluN3A accelerates the expression of markers of synaptic maturation (Henson et al., 2012). Faster synaptic maturation could result from the loss of GluN1/GluN2B/GluN3A heterotrimers and the insertion of GluN2A-containing NMDARs. This scenario is further supported by the observation that, in the VTA, neonatal synapses onto DA neurons are characterized by Ca^{2+}-impermeable NMDARs with high ifenprodil sensitivity and slow decay time kinetics (Bellone et al., 2011). We therefore favor a scenario where at neonatal synapses after the birth, NMDAR synaptic transmission is mediated by GluN3A- and GluN2B-containing subunits that are replaced by GluN2A-containing ones

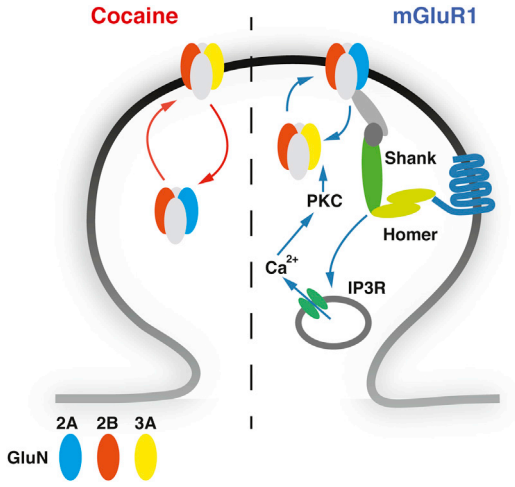

Figure 8. Model for Cocaine-Evoked Plasticity of NMDARs and mGluR1-Induced Reversal

After a single cocaine injection (red arrows), GluN2B/GluN2A-containing NMDARs are removed from synapses and GluN2B/GluN3A-containing NMDARs are inserted. The pharmacological activation of mGluR1 (blue arrows), restores basal synaptic transmission promoting the removal of nonconventional NMDARs and the insertion of GluN2A-containing NMDARs at the synapses via Shank3/Homer interaction, Ca^{2+} release from internal store, and PKC activation.

within the third postnatal week. At juvenile and adult synapses, a single cocaine injection triggers receptor redistribution with the reappearance of subunits typically present in immature synapses. Such observations lead us to propose that addictive drugs may reopen a critical period of synapse development (Bellone and Lüscher, 2012).

The role of mGluR1s in orchestrating both AMPARs and NMDARs is of particular interest. We have previously shown that mGluR1 drives the postnatal maturation of AMPARs and NMDARs (Bellone et al., 2011). In the present study we show that mGluR1 activation restores baseline transmission after cocaine exposure. mGluR1-mediated restoration of baseline transmission is not limited to NMDARs in the VTA, but may also provide an efficient mechanism to reverse cocaine-evoked plasticity in other brain structures within the mesocorticolimbic system (Mameli et al., 2007, 2009; McCutcheon et al., 2011; Loweth et al., 2013). Collectively, these data point to mGluR1 as an important modulator of the synaptic transmission and a potential target for drug development (Loweth et al., 2013). In the present study, we have explored the signaling pathway recruited following mGluR1 stimulation. Interestingly, both mGluR1-driven AMPAR and NMDAR redistribution share a common signaling pathway that involves Homer/Shank and mTOR. A number of other signaling molecules may also be important in this phenomenon. For example, in culture systems, endocytic removal of GluN3A is regulated by PACSIN1/syndapin1 (Pérez-Otaño et al., 2006). PACSIN contains several potential phosphorylation sites for PKC and casein kinase 2 (Plomann et al., 1998), both of which are implicated in NMDAR subunit regulation (Sanz-Clemente et al., 2010). Since mGluR1 activation drives the removal of GluN3A-containing and the insertion of GluN2A-containing NMDARs via a Ca^{2+}-dependent pathway, it will be of interest to investigate whether mGluR1 activation recruits PACSIN to promote GluN3A endocytosis.

What might be the functional consequences of changing NMDAR subunit composition for subsequent activity-dependent synaptic plasticity? It has previously been proposed that the GluN2A/2B ratio of NMDARs determines whether given neuronal activity induces LTP or LTD (Liu et al., 2004). This simple concept has been challenged (Berberich et al., 2005; Morishita et al., 2007) and a more likely scenario is that GluN2A and GluN2B are both involved in potentiation and depression of synaptic transmission. While GluN2A-containing NMDARs are responsible for Ca^{2+} influx, GluN2B subunits would play a crucial role in LTP expression (Foster et al., 2010). GluN3A could also modulate synaptic plasticity, suggesting that the expression of this subunit prevents the induction of synaptic potentiation (Roberts et al., 2009). While the amplitudes of NMDAR-EPSCs in dissociated cortical neurons from GluN3A KO mice are increased (Das et al., 1998), the ratio of the NMDAR- to AMPAR-EPSCs is higher in GluN3A KO mice than in WT mice (Tong et al., 2008). These data may reflect a larger NMDAR component, suggesting that GluN3A can affect the synaptic transmission in a naive system (Tong et al., 2008).

With respect to DA neurons of the VTA, cocaine exposure drives the redistribution of both NMDARs and AMPARs (Schilström et al., 2006; Bellone and Lüscher, 2006; Argilli et al., 2008; Conrad et al., 2008; Mameli et al., 2011), which profoundly affects excitatory transmission. For example, pairing presynaptic stimulation of glutamatergic afferents with postsynaptic burst firing of DA neurons leads to an LTP of the NMDAR-EPSCS (Harnett et al., 2009), which is enhanced after amphetamine (Ahn et al., 2010) or ethanol exposure (Bernier et al., 2011). In baseline conditions, GluN2A-containing NMDARs are Ca^{2+} permeable. After cocaine exposure, these NMDAR subtypes are replaced by GluN2B/GluN3A-containing NMDARs, in parallel with the insertion of GluA2-lacking CP-AMPARs (Bellone and Lüscher, 2006). The source of synaptic Ca^{2+} switches from NMDAR to AMPAR dependent. As a consequence, the most efficient protocol to promote synaptic Ca^{2+} entry shifts from depolarization through canonical NMDARs to hyperpolarization of the Ca^{2+}-permeable AMPARs. In line with this prediction, the typical NMDAR-dependent LTP of AMPARs is also absent after cocaine (Argilli et al., 2008; Luu and Malenka, 2008; Mameli et al., 2011), probably due to a change in NMDARs that are no longer able to induce plasticity.

The observation that targeted deletion of GluN3A abolished the cocaine-driven NMDA subunit redistribution indicates that GluN3A is necessary for the expression of cocaine-evoked plasticity of both AMPAR- and NMDAR-mediated transmission. A critical step will be to understand the role for GluN3 in behavioral changes triggered by cocaine experience. Previous studies have explored the link between cocaine-evoked plasticity and addiction-relevant behaviors (Engblom et al., 2008; Mameli et al., 2009). Notably, deletion of the GluN1 subunit specifically in dopamine neurons, using a NR1 floxed x DAT cre mouse line, was found to impair reinstatement of cocaine seeking in both conditioned place preference and drug self-administration paradigms (Engblom et al., 2008; Zweifel et al., 2008; Mameli et al.,

2009). In light of our findings, one possibility is that impaired reinstatement was due in part to a loss of GluN3-containing NMDAR subunits in VTA neurons. Although we saw no differences in both behavioral sensitization to cocaine and CPP using an ShRNA approach, we might predict that GluN3A plays an important role in the ability of cocaine-associated stimuli to trigger relapse to drug seeking.

The tight coupling of NMDAR and AMPAR redistribution also raises the possibility that at other synapses, where GluA2-lacking AMPARs have been observed, the NMDA transmission may be affected. For example, CP-AMPARs are present at excitatory synapses onto interneurons in the cortex and hippocampus (Liu and Zukin, 2007). In these cells, an anti-Hebbian form of LTP that is induced by Ca^{2+} entering the cells through AMPARs can be observed (Lamsa et al., 2007). Whether Ca^{2+}-impermeable NMDAR are also present at these synapses has not been investigated. As described above, both CP-AMPARs and GluN3A-containing NMDARs are present at many synapses during the early postnatal development (Ho et al., 2007; Henson et al., 2010; Bellone et al., 2011) and may be permissive for circuit formation in the developing brain and for activity-dependent changes in the mature brain.

Regardless of the identity of the molecular linker, the subunit switch for NMDARs and AMPARs represents a form of metaplasticity. Rather than encoding specific events, cocaine sets the rules for subsequent activity-dependent synaptic plasticity (Mameli et al., 2011). After cocaine, NMDAR activation no longer induces LTP (because of the insignificant Ca^{2+} permeability), which, however, can be rescued when hyperpolarizing the cell during the induction protocol (thus favoring Ca^{2+} entry via GluA2-lacking inwardly rectifiying AMPARs). Through this switch, cocaine-evoked synaptic plasticity of excitatory transmission in the VTA plays a permissive role for circuit adaptations in target regions (Mameli et al., 2009). Boosting mGluR1s, for example with positive allosteric modulators to remove GluN3-containing NMDARs, may ultimately restore normal synaptic transmission, prevent adaptations in downstream circuits, and stop the development of addiction.

EXPERIMENTAL PROCEDURES

Animals

C57/BL6 mice (male and female) and NR3A heterozygotes and knockouts were injected with cocaine (15 mg/kg i.p.) or the same volume of saline as controls. The dose of cocaine that we used did not induce seizures or increase mortality. The study was conducted in accordance with the Institutional Animal Care and Use Committee of the University of Geneva and with permission of the cantonal authorities (Permit No. 1007/3592/2).

Electrophysiology

The majority of electrophysiology recordings were undertaken in young mice (P14–40) to facilitate identification of VTA cells. However, note that maturation of excitatory transmission in the VTA of mice is complete at P14 (Bellone et al., 2011) and we have also reported cocaine-evoked plasticity of VTA DA neuron excitatory synapses in adult mice (aged 7 months, Mameli et al., 2009). After animals were sacrificed, 250-μm-thick horizontal midbrain slices containing the VTA were prepared and whole-cell voltage-clamp recordings were made as previously shown (Bellone and Lüscher, 2006). The access resistance was monitored by a hyperpolarizing step of −14 mV with each sweep, every 10 s. The cells were recorded at the access resistance from 10–25 MΩ, and data were excluded when the resistance changed > 20%. Synaptic currents were evoked by stimuli (0.05–0.1 ms) at 0.1 Hz through a stimulating electrode placed rostral to the VTA. The experiments were carried out in the presence of $GABA_A$ receptor antagonist picrotoxin (100 μM); the AMPAR EPSCs were pharmacologically isolated by application of the NMDARs antagonist D, L-APV (100 μM), whereas the NMDA EPSCs were pharmacologically isolated by the application of the AMPARs antagonist NBQX (10 μM). Representative example traces are shown as the average of 20 consecutive EPSCs typically obtained at each potential or, in the case of plasticity protocols, during the last 5 min of the baseline and at least 30 min after the induction of plasticity. The decay time τ_w of NMDA EPSC was calculated as described previously (Bellone and Nicoll, 2007). The rectification index of AMPARs is the ratio of the chord conductance calculated at negative potential divided by the chord conductance at positive potentials. I-V curves of pharmacologically isolated NMDARs were generated holding the cells at different membrane potential for 5 min each and normalizing EPSCs at 40 mV. Tricine (*N*-tris(hydroxymethyl)methylglycine, 10 mM) was used to buffer zinc following the relationship [Zn]free = [Zn]added/200 (Paoletti et al., 1997).

All drugs were purchased from Tocris, except Tetanus Toxin that was purchased from Sigma Aldrich. The peptides were synthetized by China Peptides with 95% purity and TFA was transferred to phosphate for neutral pH (Shanghai, China).

RNA Interference

A 59 bp fragment encoding a 19-bp-long small hairpin RNA (shRNA) specific for rat and mouse GluN3A (sh-GluN3A target sequence: CTACAGCTGAGTT TAGAAA) was used. Selectivity was tested in cultured cortical neurons infected with viral vectors expressing the sh-GluN3A by immunoblot quantification of endogenous levels of GluN3A and other neuronal proteins. Cultured neurons were collected in lysis buffer containing Tris 50 mM, EDTA 2 mM, and 1% TX-100 and supplemented with protease inhibitors (Roche Complete). Proteins in the lysate were separated by SDS-PAGE and transferred onto PVDF membranes, and membranes were probed with the following primary antibodies: anti-GluN3A (Millipore, 1:1000), anti-GluN2B (NeuroMab, clone N59/20, 1:100), anti-GluA1 (Chemicon, 1:1000), anti-GluN2A (Millipore, clone AW12, 1:1000), anti-PSD-95 (Millipore, 1:10000), and anti-tubulin (Sigma, 1:10000).

Stereotaxic Injection

Injections of purified AAV5-shRNA-GFP were performed in 2-week-old mice. The animals were anesthetized and maintained with isoflurane (Baxter AG, Vienna, Austria) at 5% and 1% (in oxygen), respectively. The animals were then placed on the stereotaxic frame (Angle One; Leica, Germany) and unilateral craniotomy were made over the VTA at following stereotaxic coordinates (ML 0.5 to 0.6, AP −3, DV 4.2 from Bregma). The virus was injected with graduated pipettes (Drummond Scientific Company, Broomall, PA) (tip diameter of 10–15 μm) at the rate of ~100 nl/min for a total volume of 500 nl. In all experiments the virus was allowed a 15–20 days to incubate before any other procedures were carried out.

Behavioral Experiments

Wild-type C57BL6 mice aged 4–5 weeks at study starts were bilaterally injected with a virus expressing shGluN3A or GFP (n = 8) into the VTA. Three weeks after the infection, mice were exposed to a nonbiased three-chamber CPP procedure comprising a single 20 min preconditioning test (pre) followed by four once-daily cocaine (10 mg/kg i.p.) and four once-daily saline 30 min conditioning sessions (alternating order) and finally a single 20 min postconditioning test (post). Locomotor activity was video tracked and analyzed with ANY-maze behavioral software (Stoelting, Illinois, USA).

Immunohistochemistry

The animals were sacrificed and transcardially perfused with 0.01 M PBS followed by 4% paraformaldehyde in phosphate buffer. The brain was then removed and left for overnight postfixation at 4°C. Horizontal VTA slices were cut at 50 μm and washed three times in PBS before incubation in the blocking solution containing 0.3% triton, 5% BSA, and 2% goat serum. Then the slices were incubated with rabbit anti-TH (Millipore, 1:500) at 4°C

overnight. The slices were washed three times in PBS before 2 hr incubation with secondary antibody goat anti-rabbit IgG-Alexa 568 (Invitrogen, 1:200). Finally, the slices were washed three times in PBS before being mounted onto the slides with Dako DAPI-mounting medium.

Calcium Imaging with Two-Photon Microscopy

Dendritic fluorescence was measured with a two-photon laser-scanning microscope based on the Olympus FV-300 system (side-mounted to a BX50WI microscope with a 40×, 0.8 NA water-immersion objective) and a Mai-Tai laser (Spectra Physics) operating at 830 nm. Green and red fluorescence signals were acquired simultaneously in line-scan mode where the line scan was oriented along the dendrite and quantified as increases in green fluorescence normalized to red fluorescence ($\Delta G/R$). Synaptic stimulation was obtained with a glass pipette located proximally to the dendrite. Neurons were voltage clamped at −60 mV to detect a mixture of AMPAR- and NMDAR-mediated responses in Mg^{2+}-free aCSF containing 100 μM picrotoxin, 50 μM mibefradil (T-type voltage-gated calcium channel [VGCC] blocker), and 100 μM nimodipine (L-type VGCC blocker). The intracellular solution contained 130 mM cesium-methanesulphonate, 10 mM HEPES, 10 mM sodium phosphocreatine, 4 mM MgCl2, 4 mM Na-ATP, 0.4 mM Na-GTP, 0.1 mM Oregon green BAPTA1, and 0.02 mM AlexaFluo Red. After obtaining the whole-cell configuration, 15–20 min were allowed for intracellular diffusion of fluorophores.

Biochemical Peptide Characterization

HEK cells were cotransfected with HA-Shank3 and Myc-Homer1b cDNAs (Romorini et al., 2004; Roussignol et al., 2005) in the mammalian expression vector pGW1-CMV using Lipofectamine 2000 (Invitrogen). Two days after transfection the cells were extracted in buffer A containing 200 mM NaCl, 10 mM EDTA, 10 mM Na_2HPO_4, 0.5% NP-40, 0.1% SDS, and protein inhibitor cocktails. For the coimmunoprecipitation, samples (100 μg proteins) were incubated overnight at 4°C with antibodies (rabbit anti-HA antibodies 1:200, Roche Applied Science) in presence of 100 μM dominant-negative peptide (dnShank3) LVPPPEFAN or scrambled peptide (scShank3) PANFLPVPE. Protein A agarose beads (Santa Cruz Biotechnology) washed in the same buffer were added, and incubation continued for 2 hr. The beads were collected by centrifugation and washed five times with buffer A. Samples were resuspended in sample buffer for SDS-PAGE, and the mixture was boiled for 5 min. Beads were pelleted by centrifugation, and supernatants were applied to 7.5% or 10% SDS-PAGE. The following antibodies were used: goat anti-iL1RAPL1 (R&D Systems) at dilution 1:1000, mouse anti-HA (Santa Cruz Biotechnology), rabbit anti-Myc-tag (Santa Cruz Biotechnology), and mouse anti-HA-tag (Roche Applied Science).

SUPPLEMENTAL INFORMATION

Supplemental Information includes six figures and can be found with this article online at http://dx.doi.org/10.1016/j.neuron.2013.07.050.

AUTHOR CONTRIBUTIONS

T.Y., C.B., and M.M. carried out all electrophysiology experiments. T.Y and M.M carried out the Ca^{2+} imaging experiments. C.S. and C.V. carried out the peptide characterization. E.O.C. carried out all the behavioral experiments. I.P.O. and P.N.D. carried out the ShGluN3A characterization. C.B. designed the study with C.L. and M.M. and wrote the manuscript with E.O.C. and C.L.

ACKNOWLEDGMENTS

We thank members of the Lüscher laboratory, Matthew Brown, and Alexander Jackson for helpful discussions and suggestions regarding the manuscript. GluN3A knockout mice were kindly provided by Nobuki Nakanishi and Stuart Lipton. We thank Bernard Schneider (Brain and Mind Institute, EPFL) for the virus production. We thank Agnes Hiver for assistance with surgery and Francoise Loctin for technical support. T.Y. is supported by Symbad, a Marie Curie training grant of the European Community. C.L. is supported by grants from the Swiss National Science Foundation, SFARI (Simons foundation), and the European Research Council (MeSSI Advanced grant). I.P.O. is supported by grants from the UTE project CIMA, NARSAD, and Spanish Ministry of Science (SAF2010-20636 and CSD2008-00005). C.B. is supported by Ambizione program of the Swiss National Science Foundation. C.S. is supported by Telethon Fondazione Onlus, grant GGP11095 and PNR-CNR Aging Program 2012–2014 and Ministry of Health in the frame of ERA-NET NEURON.

Accepted: July 30, 2013
Published: October 31, 2013

REFERENCES

Ahn, K.C., Bernier, B.E., Harnett, M.T., and Morikawa, H. (2010). IP3 receptor sensitization during in vivo amphetamine experience enhances NMDA receptor plasticity in dopamine neurons of the ventral tegmental area. J. Neurosci. *30*, 6689–6699.

Al-Hallaq, R.A., Jarabek, B.R., Fu, Z., Vicini, S., Wolfe, B.B., and Yasuda, R.P. (2002). Association of NR3A with the *N*-methyl-D-aspartate receptor NR1 and NR2 subunits. Mol. Pharmacol. *62*, 1119–1127.

Al-Hallaq, R.A., Conrads, T.P., Veenstra, T.D., and Wenthold, R.J. (2007). NMDA di-heteromeric receptor populations and associated proteins in rat hippocampus. J. Neurosci. *27*, 8334–8343.

Anggono, V., and Huganir, R.L. (2012). Regulation of AMPA receptor trafficking and synaptic plasticity. Curr. Opin. Neurobiol. *22*, 461–469.

Argilli, E., Sibley, D.R., Malenka, R.C., England, P.M., and Bonci, A. (2008). Mechanism and time course of cocaine-induced long-term potentiation in the ventral tegmental area. J. Neurosci. *28*, 9092–9100.

Bellone, C., and Lüscher, C. (2006). Cocaine triggered AMPA receptor redistribution is reversed in vivo by mGluR-dependent long-term depression. Nat. Neurosci. *9*, 636–641.

Bellone, C., and Lüscher, C. (2012). Drug-evoked plasticity: do addictive drugs reopen a critical period of postnatal synaptic development? Front. Mol. Neurosci. *5*, 75.

Bellone, C., and Nicoll, R.A. (2007). Rapid bidirectional switching of synaptic NMDA receptors. Neuron *55*, 779–785.

Bellone, C., Lüscher, C., and Mameli, M. (2008). Mechanisms of synaptic depression triggered by metabotropic glutamate receptors. Cell. Mol. Life Sci. *65*, 2913–2923.

Bellone, C., Mameli, M., and Lüscher, C. (2011). In utero exposure to cocaine delays postnatal synaptic maturation of glutamatergic transmission in the VTA. Nat. Neurosci. *14*, 1439–1446.

Berberich, S., Punnakkal, P., Jensen, V., Pawlak, V., Seeburg, P.H., Hvalby, Ø., and Köhr, G. (2005). Lack of NMDA receptor subtype selectivity for hippocampal long-term potentiation. J. Neurosci. *25*, 6907–6910.

Bernier, B.E., Whitaker, L.R., and Morikawa, H. (2011). Previous ethanol experience enhances synaptic plasticity of NMDA receptors in the ventral tegmental area. J. Neurosci. *31*, 5205–5212.

Bloodgood, B.L., Giessel, A.J., and Sabatini, B.L. (2009). Biphasic synaptic Ca influx arising from compartmentalized electrical signals in dendritic spines. PLoS Biol. *7*, e1000190.

Brown, M.T.C., Bellone, C., Mameli, M., Labouèbe, G., Bocklisch, C., Balland, B., Dahan, L., Luján, R., Deisseroth, K., and Lüscher, C. (2010). Drug-driven AMPA receptor redistribution mimicked by selective dopamine neuron stimulation. PLoS ONE *5*, e15870.

Conrad, K.L., Tseng, K.Y., Uejima, J.L., Reimers, J.M., Heng, L.-J., Shaham, Y., Marinelli, M., and Wolf, M.E. (2008). Formation of accumbens GluR2-lacking AMPA receptors mediates incubation of cocaine craving. Nature *454*, 118–121.

Cull-Candy, S.G., and Leszkiewicz, D.N. (2004). Role of distinct NMDA receptor subtypes at central synapses. Sci. STKE *2004*, re16.

Das, S., Sasaki, Y.F., Rothe, T., Premkumar, L.S., Takasu, M., Crandall, J.E., Dikkes, P., Conner, D.A., Rayudu, P.V., Cheung, W., et al. (1998). Increased

NMDA current and spine density in mice lacking the NMDA receptor subunit NR3A. Nature *393*, 377–381.

Engblom, D., Bilbao, A., Sanchis-Segura, C., Dahan, L., Perreau-Lenz, S., Balland, B., Parkitna, J.R., Luján, R., Halbout, B., Mameli, M., et al. (2008). Glutamate receptors on dopamine neurons control the persistence of cocaine seeking. Neuron *59*, 497–508.

Foster, K.A., McLaughlin, N., Edbauer, D., Phillips, M., Bolton, A., Constantine-Paton, M., and Sheng, M. (2010). Distinct roles of NR2A and NR2B cytoplasmic tails in long-term potentiation. J. Neurosci. *30*, 2676–2685.

Gray, J.A., Shi, Y., Usui, H., During, M.J., Sakimura, K., and Nicoll, R.A. (2011). Distinct modes of AMPA receptor suppression at developing synapses by GluN2A and GluN2B: single-cell NMDA receptor subunit deletion in vivo. Neuron *71*, 1085–1101.

Harnett, M.T., Bernier, B.E., Ahn, K.-C., and Morikawa, H. (2009). Burst-timing-dependent plasticity of NMDA receptor-mediated transmission in midbrain dopamine neurons. Neuron *62*, 826–838.

Hayashi, M.K., Tang, C., Verpelli, C., Narayanan, R., Stearns, M.H., Xu, R.-M., Li, H., Sala, C., and Hayashi, Y. (2009). The postsynaptic density proteins Homer and Shank form a polymeric network structure. Cell *137*, 159–171.

Henson, M.A., Roberts, A.C., Pérez-Otaño, I., and Philpot, B.D. (2010). Influence of the NR3A subunit on NMDA receptor functions. Prog. Neurobiol. *91*, 23–37.

Henson, M.A., Larsen, R.S., Lawson, S.N., Pérez-Otaño, I., Nakanishi, N., Lipton, S.A., and Philpot, B.D. (2012). Genetic deletion of NR3A accelerates glutamatergic synapse maturation. PLoS ONE *7*, e42327.

Ho, M.T.W., Pelkey, K.A., Topolnik, L., Petralia, R.S., Takamiya, K., Xia, J., Huganir, R.L., Lacaille, J.C., and McBain, C.J. (2007). Developmental expression of Ca2+-permeable AMPA receptors underlies depolarization-induced long-term depression at mossy fiber CA3 pyramid synapses. J. Neurosci. *27*, 11651–11662.

Kauer, J.A., and Malenka, R.C. (2007). Synaptic plasticity and addiction. Nat. Rev. Neurosci. *8*, 844–858.

Kwon, H.-B., and Castillo, P.E. (2008). Long-term potentiation selectively expressed by NMDA receptors at hippocampal mossy fiber synapses. Neuron *57*, 108–120.

Lamsa, K.P., Heeroma, J.H., Somogyi, P., Rusakov, D.A., and Kullmann, D.M. (2007). Anti-Hebbian long-term potentiation in the hippocampal feedback inhibitory circuit. Science *315*, 1262–1266.

Lau, C.G., and Zukin, R.S. (2007). NMDA receptor trafficking in synaptic plasticity and neuropsychiatric disorders. Nat. Rev. Neurosci. *8*, 413–426.

Lau, C.G., Takayasu, Y., Rodenas-Ruano, A., Paternain, A.V., Lerma, J., Bennett, M.V.L., and Zukin, R.S. (2010). SNAP-25 is a target of protein kinase C phosphorylation critical to NMDA receptor trafficking. J. Neurosci. *30*, 242–254.

Liu, S.J., and Zukin, R.S. (2007). Ca2+-permeable AMPA receptors in synaptic plasticity and neuronal death. Trends Neurosci. *30*, 126–134.

Liu, L., Wong, T.P., Pozza, M.F., Lingenhoehl, K., Wang, Y., Sheng, M., Auberson, Y.P., and Wang, Y.T. (2004). Role of NMDA receptor subtypes in governing the direction of hippocampal synaptic plasticity. Science *304*, 1021–1024.

Loweth, J.A., Tseng, K.Y., and Wolf, M.E. (2013). Using metabotropic glutamate receptors to modulate cocaine's synaptic and behavioral effects: mGluR1 finds a niche. Curr. Opin. Neurobiol. *23*, 500–506.

Lüscher, C., and Huber, K.M. (2010). Group 1 mGluR-dependent synaptic long-term depression: mechanisms and implications for circuitry and disease. Neuron *65*, 445–459.

Lüscher, C., and Malenka, R.C. (2011). Drug-evoked synaptic plasticity in addiction: from molecular changes to circuit remodeling. Neuron *69*, 650–663.

Luu, P., and Malenka, R.C. (2008). Spike timing-dependent long-term potentiation in ventral tegmental area dopamine cells requires PKC. J. Neurophysiol. *100*, 533–538.

Mameli, M., Balland, B., Luján, R., and Lüscher, C. (2007). Rapid synthesis and synaptic insertion of GluR2 for mGluR-LTD in the ventral tegmental area. Science *317*, 530–533.

Mameli, M., Halbout, B., Creton, C., Engblom, D., Parkitna, J.R., Spanagel, R., and Lüscher, C. (2009). Cocaine-evoked synaptic plasticity: persistence in the VTA triggers adaptations in the NAc. Nat. Neurosci. *12*, 1036–1041.

Mameli, M., Bellone, C., Brown, M.T.C., and Lüscher, C. (2011). Cocaine inverts rules for synaptic plasticity of glutamate transmission in the ventral tegmental area. Nat. Neurosci. *14*, 414–416.

Matta, J.A., Ashby, M.C., Sanz-Clemente, A., Roche, K.W., and Isaac, J.T.R. (2011). mGluR5 and NMDA receptors drive the experience- and activity-dependent NMDA receptor NR2B to NR2A subunit switch. Neuron *70*, 339–351.

McCutcheon, J.E., Wang, X., Tseng, K.Y., Wolf, M.E., and Marinelli, M. (2011). Calcium-permeable AMPA receptors are present in nucleus accumbens synapses after prolonged withdrawal from cocaine self-administration but not experimenter-administered cocaine. J. Neurosci. *31*, 5737–5743.

Monyer, H., Burnashev, N., Laurie, D.J., Sakmann, B., and Seeburg, P.H. (1994). Developmental and regional expression in the rat brain and functional properties of four NMDA receptors. Neuron *12*, 529–540.

Morishita, W., Lu, W., Smith, G.B., Nicoll, R.A., Bear, M.F., and Malenka, R.C. (2007). Activation of NR2B-containing NMDA receptors is not required for NMDA receptor-dependent long-term depression. Neuropharmacology *52*, 71–76.

Mullasseril, P., Hansen, K.B., Vance, K.M., Ogden, K.K., Yuan, H., Kurtkaya, N.L., Santangelo, R., Orr, A.G., Le, P., Vellano, K.M., et al. (2010). A subunit-selective potentiator of NR2C- and NR2D-containing NMDA receptors. Nat. Commun. *1*, 90.

Pachernegg, S., Strutz-Seebohm, N., and Hollmann, M. (2012). GluN3 subunit-containing NMDA receptors: not just one-trick ponies. Trends Neurosci. *35*, 240–249.

Paoletti, P. (2011). Molecular basis of NMDA receptor functional diversity. Eur. J. Neurosci. *33*, 1351–1365.

Paoletti, P., Ascher, P., and Neyton, J. (1997). High-affinity zinc inhibition of NMDA NR1-NR2A receptors. J. Neurosci. *17*, 5711–5725.

Paoletti, P., Bellone, C., and Zhou, Q. (2013). NMDA receptor subunit diversity: impact on receptor properties, synaptic plasticity and disease. Nat. Rev. Neurosci. *14*, 383–400.

Perez-Otano, I., Schulteis, C.T., Contractor, A., Lipton, S.A., Trimmer, J.S., Sucher, N.J., and Heinemann, S.F. (2001). Assembly with the NR1 subunit is required for surface expression of NR3A-containing NMDA receptors. J. Neurosci. *21*, 1228–1237.

Pérez-Otaño, I., Luján, R., Tavalin, S.J., Plomann, M., Modregger, J., Liu, X.B., Jones, E.G., Heinemann, S.F., Lo, D.C., and Ehlers, M.D. (2006). Endocytosis and synaptic removal of NR3A-containing NMDA receptors by PACSIN1/syndapin1. Nat. Neurosci. *9*, 611–621.

Plomann, M., Lange, R., Vopper, G., Cremer, H., Heinlein, U.A., Scheff, S., Baldwin, S.A., Leitges, M., Cramer, M., Paulsson, M., and Barthels, D. (1998). PACSIN, a brain protein that is upregulated upon differentiation into neuronal cells. Eur. J. Biochem. *256*, 201–211.

Rebola, N., Lujan, R., Cunha, R.A., and Mulle, C. (2008). Adenosine A2A receptors are essential for long-term potentiation of NMDA-EPSCs at hippocampal mossy fiber synapses. Neuron *57*, 121–134.

Roberts, A.C., Díez-García, J., Rodriguiz, R.M., López, I.P., Luján, R., Martínez-Turrillas, R., Picó, E., Henson, M.A., Bernardo, D.R., Jarrett, T.M., et al. (2009). Downregulation of NR3A-containing NMDARs is required for synapse maturation and memory consolidation. Neuron *63*, 342–356.

Romorini, S., Piccoli, G., Jiang, M., Grossano, P., Tonna, N., Passafaro, M., Zhang, M., and Sala, C. (2004). A functional role of postsynaptic density-95-guanylate kinase-associated protein complex in regulating Shank assembly and stability to synapses. J. Neurosci. *24*, 9391–9404.

Roussignol, G., Ango, F., Romorini, S., Tu, J.C., Sala, C., Worley, P.F., Bockaert, J., and Fagni, L. (2005). Shank expression is sufficient to induce

functional dendritic spine synapses in aspiny neurons. J. Neurosci. *25*, 3560–3570.

Sala, C., Roussignol, G., Meldolesi, J., and Fagni, L. (2005). Key role of the postsynaptic density scaffold proteins Shank and Homer in the functional architecture of Ca2+ homeostasis at dendritic spines in hippocampal neurons. J. Neurosci. *25*, 4587–4592.

Sanchez, J.T., Wang, Y., Rubel, E.W., and Barria, A. (2010). Development of glutamatergic synaptic transmission in binaural auditory neurons. J. Neurophysiol. *104*, 1774–1789.

Sans, N., Petralia, R.S., Wang, Y.X., Blahos, J., 2nd, Hell, J.W., and Wenthold, R.J. (2000). A developmental change in NMDA receptor-associated proteins at hippocampal synapses. J. Neurosci. *20*, 1260–1271.

Sanz-Clemente, A., Matta, J.A., Isaac, J.T.R., and Roche, K.W. (2010). Casein kinase 2 regulates the NR2 subunit composition of synaptic NMDA receptors. Neuron *67*, 984–996.

Sanz-Clemente, A., Nicoll, R.A., and Roche, K.W. (2012). Diversity in NMDA Receptor Composition: Many Regulators, Many Consequences. Neuroscientist *19*, 62–75.

Schilström, B., Yaka, R., Argilli, E., Suvarna, N., Schumann, J., Chen, B.T., Carman, M., Singh, V., Mailliard, W.S., Ron, D., and Bonci, A. (2006). Cocaine enhances NMDA receptor-mediated currents in ventral tegmental area cells via dopamine D5 receptor-dependent redistribution of NMDA receptors. J. Neurosci. *26*, 8549–8558.

Sheng, M., Cummings, J., Roldan, L.A., Jan, Y.N., and Jan, L.Y. (1994). Changing subunit composition of heteromeric NMDA receptors during development of rat cortex. Nature *368*, 144–147.

Sobczyk, A., Scheuss, V., and Svoboda, K. (2005). NMDA receptor subunit-dependent [Ca2+] signaling in individual hippocampal dendritic spines. J. Neurosci. *25*, 6037–6046.

Tong, G., Takahashi, H., Tu, S., Shin, Y., Talantova, M., Zago, W., Xia, P., Nie, Z., Goetz, T., Zhang, D., et al. (2008). Modulation of NMDA receptor properties and synaptic transmission by the NR3A subunit in mouse hippocampal and cerebrocortical neurons. J. Neurophysiol. *99*, 122–132.

Traynelis, S.F., Wollmuth, L.P., McBain, C.J., Menniti, F.S., Vance, K.M., Ogden, K.K., Hansen, K.B., Yuan, H., Myers, S.J., and Dingledine, R. (2010). Glutamate receptor ion channels: structure, regulation, and function. Pharmacol. Rev. *62*, 405–496.

Ungless, M.A., Whistler, J.L., Malenka, R.C., and Bonci, A. (2001). Single cocaine exposure in vivo induces long-term potentiation in dopamine neurons. Nature *411*, 583–587.

Verpelli, C., and Sala, C. (2012). Molecular and synaptic defects in intellectual disability syndromes. Curr. Opin. Neurobiol. *22*, 530–536.

Williams, K., Russell, S.L., Shen, Y.M., and Molinoff, P.B. (1993). Developmental switch in the expression of NMDA receptors occurs in vivo and in vitro. Neuron *10*, 267–278.

Wong, H.-K., Liu, X.-B., Matos, M.F., Chan, S.F., Pérez-Otaño, I., Boysen, M., Cui, J., Nakanishi, N., Trimmer, J.S., Jones, E.G., et al. (2002). Temporal and regional expression of NMDA receptor subunit NR3A in the mammalian brain. J. Comp. Neurol. *450*, 303–317.

Zweifel, L.S., Argilli, E., Bonci, A., and Palmiter, R.D. (2008). Role of NMDA receptors in dopamine neurons for plasticity and addictive behaviors. Neuron *59*, 486–496.